Analysis of Translational Ship Oscillations in a Realistic Environment

Chen Zhang, Bernhard Schwarz-Röhr, Alexander Härting

Abstract—To acquire accurate ship motions at the center of gravity, a single low-cost inertial sensor is utilized and applied on board to measure ship oscillating motions. As observations, the three axes accelerations and three axes rotational rates provided by the sensor are used. The mathematical model of processing the observation data includes determination of the distance vector between the sensor and the center of gravity in x, y, and z directions. After setting up the transfer matrix from sensor's own coordinate system to the ship's body frame, an extended Kalman filter is applied to deal with nonlinearities between the ship motion in the body frame and the observation information in the sensor's frame. As a side effect, the method eliminates sensor noise and other unwanted errors. Results are not only roll and pitch, but also linear motions, in particular heave and surge at the center of gravity. For testing, we resort to measurements recorded on a small vessel in a well-defined sea state. With response amplitude operators computed numerically by a commercial software (Seaway), motion characteristics are estimated. These agree well with the measurements after processing with the suggested method.

Keywords—Extended Kalman filter, nonlinear estimation, sea trial, ship motion estimation.

I. Introduction

DUE to influence from wind and waves, a vessel exhibits oscillating motions in six degrees of freedom (DOFs). As shown in Fig. 1, the translational motions are surge (longitudinal), sway (lateral), and heave (vertical). The rotational DOFs are roll (rotation about the longitudinal axis), pitch (about the transverse axis), and yaw (about the vertical axis) [1]. The motions can be recorded by instruments, such as inertial measurement unit (IMU), accelerometer, gyroscope, GPS and magnetometer, etc. Accelerometers measure the linear accelerations in the body-fixed coordinate system, and gyroscopes collect the rotational rates. To obtain the linear elongations and attitude angles of a ship, the accelerometer signals need to be integrated twice, while the gyroscope signals need one integration. Because of sensor errors, for example measured noise and bias, the integrated signals contain an increasing drift in position and attitude, which must be removed by some high-pass filter to acquire the true motion information. This paper focuses on the estimation of heave and surge motions at the center of gravity (CG) as a reference point. Due to uncertainties in the mass distribution (cargo, fuel, ballast

etc.), the position of CG is only known approximately. If a single IMU is employed for measurement, it would be desirable to place it at CG of the ship. However, this is usually not possible, and the offset vector is hard to pre-determine.

In the approach presented here, the sensor's raw data are processed to obtain the measurements in the ship body-fixed coordinate system. The offset vector, with components defined as $[r_x, r_y, r_z]$, between the center of gravity and the sensor position is considered in the measurement model equations. Then, filter algorithms like Kalman filter or its derived methods are used to eliminate noise and other unwanted influences from the data. The resulting heave and surge motions at CG can then be analyzed depending on the offset values. For a full-scale experiment, where also data from a near-by wave buoy were available, the measurement results are compared with the expected motions in the frequency domain.
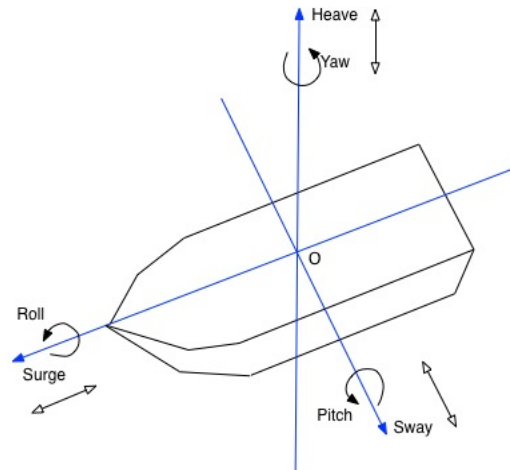

Fig. 1 Ship motion in six DOFs

II. Mathematic Observation Model

The coordinate of sensor box is the same as body frame, so in order to get the ship motion information, Euler transformation between body frame and inertial frame should be adopted. The Euler angles are: roll angle – Φ, pitch angle – θ, and yaw angle – ψ.

1) Euler angle transformation of linear acceleration from inertial frame to body coordinate is shown in (1).

$$R_n^b = R_\phi \cdot R_\theta \cdot R_\psi \qquad (1)$$

where R_n^b denotes the transformation matrix with Euler angle, and R_ϕ, R_θ, R_ψ are rotation matrix around x, y and z axis

Chen Zhang is with the University of Oldenburg, Oldenburg, 26129 Germany, and Jade University of Applied Science, Elsfleth, 26931 Germany (phone: +49 4404-9288-4321; e-mail: chen.zhang@uni-oldenburg.de).

Bernhard Schwarz-Röhr is with Jade University of Applied Science, Elsfleth, 26931 Germany, and Ghent University, Ghent, 9000 Belgium (e-mail: bernhard.schwarz-roehr@jade-hs.de).

Alexander Härting is with Jade University of Applied Science, Elsfleth, 26931 Germany (e-mail: haerting@jade-hs.de).

respectively,

$$R_\phi = \begin{pmatrix} 1 & 0 & 0 \\ 0 & cos\phi & sin\phi \\ 0 & -sin\phi & cos\phi \end{pmatrix} \quad (2)$$

$$R_\theta = \begin{pmatrix} cos\theta & 0 & -sin\theta \\ 0 & 1 & 0 \\ sin\theta & 0 & cos\theta \end{pmatrix} \quad (3)$$

$$R_n^b = R_\phi \cdot R_\theta \cdot R_\psi = \begin{pmatrix} cos\theta cos\psi & cos\theta sin\psi & -sin\theta \\ -cos\phi sin\psi + sin\phi sin\theta cos\psi & cos\phi cos\psi + sin\phi sin\theta sin\psi & sin\phi cos\theta \\ sin\phi sin\psi + cos\phi sin\theta cos\psi & -sin\phi cos\psi + cos\phi sin\theta sin\psi & cos\phi cos\theta \end{pmatrix} \quad (5)$$

2) The accelerations caused by offsets are body fixed, and showed in (6)

$$\begin{pmatrix} ax_{off} \\ ay_{off} \\ az_{off} \end{pmatrix} = \begin{pmatrix} \ddot{\phi} \\ \ddot{\theta} \\ \ddot{\psi} \end{pmatrix} \times \begin{pmatrix} r_x \\ r_y \\ r_z \end{pmatrix} = \begin{pmatrix} \ddot{\theta}r_z \text{-} \ddot{\psi}r_y \\ \ddot{\psi}r_x \text{-} \ddot{\phi}r_z \\ \ddot{\phi}r_y \text{-} \ddot{\theta}r_x \end{pmatrix} \quad (6)$$

with $\ddot{\phi}, \ddot{\theta}, \ddot{\psi}$ denoting roll, pitch and yaw angular accelerations, and r_x, r_y, r_z denoting distance from sensor position to ship's center of gravity in three axes directions individually.

Ignore yaw motion, namely removing $\psi, \dot{\psi}, \ddot{\psi}$ in (5) and (6) by setting $\psi = 0, \dot{\psi} = 0, \ddot{\psi} = 0$, then (5) can be simplified as:

$$R_n^{b'} = \begin{pmatrix} cos\theta & 0 & -sin\theta \\ sin\phi sin\theta & cos\phi & sin\phi cos\theta \\ cos\phi sin\theta & -sin\phi & cos\phi cos\theta \end{pmatrix} \quad (7)$$

$$R_\psi = \begin{pmatrix} cos\psi & sin\psi & 0 \\ -sin\psi & cos\psi & 0 \\ 0 & 0 & 1 \end{pmatrix} \quad (4)$$

Thus, the whole transformation from inertial frame to body coordinate is multiplying (2)-(4):

Equation (6) can be simplified as:

$$\begin{pmatrix} ax_{off} \\ ay_{off} \\ az_{off} \end{pmatrix} = \begin{pmatrix} \ddot{\theta}r_z \\ -\ddot{\phi}r_z \\ \ddot{\phi}r_y \text{-} \ddot{\theta}r_x \end{pmatrix} \quad (8)$$

In conclusion, (7) and (8) are combined with the corresponding vectors, and gravity effect is considered at the same time; therefore, gravitational acceleration g is in z-direction in the inertial frame, and it should be transformed to body-fixed frame as well. The measurement equations on sensor frame can be calculated as shown below in (9), where $ax_{sensor}, ay_{sensor}, az_{sensor}$ denote the measured three axes accelerations from sensor, and x, y, z denote desired three axes accelerations at CG respectively, meanwhile g is the gravitational acceleration.

$$h = \begin{pmatrix} ax_{sensor} \\ ay_{sensor} \\ az_{sensor} \end{pmatrix} = \begin{pmatrix} \ddot{x}cos\theta \text{-} \ddot{z}sin\theta \text{-} gsin\theta + r_z\ddot{\theta} \\ \ddot{x}sin\phi sin\theta + \ddot{y}cos\phi + \ddot{z}sin\phi cos\theta + gsin\phi cos\theta \text{-} r_z\ddot{\phi} \\ \ddot{x}cos\phi sin\theta \text{-} \ddot{y}sin\phi + \ddot{z}cos\phi cos\theta + gcos\phi cos\theta + r_y\ddot{\phi} \text{-} r_x\ddot{\theta} \end{pmatrix} \quad (9)$$

III. KALMAN FILTER

Extended Kalman filter is a trusted industry standard for state estimation process, see [3]-[5]. According to the references about extended Kalman filter algorithm, and based on this paper's situation, an extended Kalman filter is constructed with a state vector consisting of accelerations in three axes direction, and meanwhile estimating offsets of three axes.

System vectors: $[ax_{CG}, ay_{CG}, az_{CG}]$, accelerations at center of gravity.

Measurement vectors: $[ax_s, ay_s, az_s]$, acceleration measured from sensor box.

The state-space model is:

$$x_k = x_{k\text{-}1} + w_k \quad (10)$$

$$z_k = h(x_k) + v_k \quad (11)$$

where the system vector transition matrix between current system vector x_k and next step vector x_{k-1} is a unitary matrix; that is to say, every step of prediction part is just a propagation of process noise. And $h(.)$ is the measurement function formulated by (9). The center of gravity referenced estimates resulting from the propagation of model can be transformed to the sensor locations using known kinematic relationships for comparison.

IV. CALCULATION OF MOTION SPECTRA FROM WAVE BUOY DATA

In this chapter, the calculation of motion spectra from the directional wave spectrum as obtained from the wave-buoy is outlined. Wave-buoy spectra are given as power spectral densities $S(,?)$, here ω denotes the frequency and α is the wave direction relative to the vessels velocity vector. Waves of a certain frequency ω pass a moving vessel at a different frequency, the encounter frequency ω_e. For deep water both frequencies are related by

$$\omega_e = \omega \left(1 - \frac{v \cos(\alpha)}{g} \omega\right) \qquad (12)$$

Here, g denotes the gravitational acceleration, v the vessels speed. A relative angle of $\alpha = 0°$ means following waves in this convention. In Fig. 2 the encounter frequency is plotted as a function of the sea-state frequency for following seas and a particular ship speed of 7.5 knots. The graph indicates that up to three values of ω from regions I, II and III may be mapped onto one value of ω_e. In the current experiment, the following waves were found in region I only.
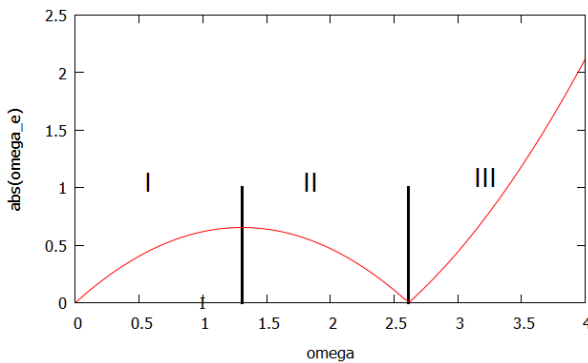

Fig. 2 Encounter frequency ω_e as a function of sea-state frequency

The encounter spectrum as $S_e(\omega_e, \alpha)$ seen by the moving vessel is related to the wave spectrum according to [2] by

$$S_e(\omega_e(\omega), \alpha) = \frac{S(\omega, \alpha)}{\left|\frac{d\omega_e}{d\omega}\right|} \qquad (13)$$

At the border between region I and II, factor $\left|\frac{d\omega_e}{d\omega}\right|$ vanishes, this creates a singularity in the encounter spectrum. Since the wave buoy spectra showed no energy in this frequency range, no measures for removing the singularity had to be taken. From the encounter spectrum, the motion spectra for the different degrees of freedom $S_i()$ can be expressed by

$$S_i(\omega_e) = |h_i(\omega_e, \alpha)|^2 \, S(\omega_e, \alpha) \qquad (14)$$

Here, i denotes the index of the degree of freedom, $h_i(\omega_e, \alpha)$ the corresponding response amplitude operator (RAO).

In this paper, the RAOs were calculated by the strip theory program PDSTRIP [6]-[8].

V. CONDUCTION OF EXPERIMENT

A. Vessel Properties

In cooperation with the Maritime Department of Cape Peninsula University of Technology (CPUT), their training vessel *Fathom 10*, a former fishery patrol boat, was made available for the experiment. The main parameters during the trials are listed in Table I. Fig. 3 shows the vessel in dry dock.

B. Environmental Conditions

The experiment was performed on 13. Feb. 2015 in open water to the West of Cape Town. In the vicinity, a wave buoy is

operated by the Council for Scientific and Industrial Research (CSIR). Waves were coming from a peak direction of about 220° with a peak period of about 11s and a significant height of about 2 m. In each experimental run, the vessel was kept on a constant heading for about 15 min and a total of five different headings were covered with 7.5 kn speed.

C. Data Acquisition

Motion data were recorded using a device (sensor box) placed laterally close to the ship's center of gravity with its axes aligned with the ship's body frame. In Fig. 4, the sensor box can be seen at the right edge of the table. Data are sent to a serial interface and/or recorded on a micro SD card. The box has two types of sensors: a 3d accelerometer and two gyros for the pitch- and roll axes, sampling at a rate of 10 Hz. After pre-processing, power spectra were calculated using a 1024 points FFT with a Hanning window and 75% overlap [9].

TABLE I
SHIP LOADING CONDITIONS

Name	Symbol	Quantity	Unit
Overall Length	L	19.6	m
Length between perpendiculars	L_{pp}	17.91	m
Breadth	B	5.0	m
Draft	T	1.64	m
Displacement	D	56.6	t
Vertical Position of center of gravity, measured from keel	KG	1.97	m
Ship velocity	v	7.5	kn

Fig. 3 Fathom 10 in dry dock

Fig. 4 Experimental setup with sensor box inside ship

VI. EXPERIMENTAL RESULTS

Via Kalman filter method, data files obtained from sensor

box onboard are processed, the linear accelerations at the position of center of gravity (CG) are acquired by filtering, afterwards surge and heave motion can be integrated from their accelerations respectively, furthermore power spectrum density distribution of each motion is generated. On the other hand, collecting wave information from wave buoy, after calculation and transformation, motion information can also be derived, further on under the condition of same heading angle and same sampling time period, to acquire corresponding ship motion power spectrum density, then compare with motion of sensor box.

A. Result Figures

Figs. 5 and 6 are power spectrum distribution (PSD) of surge and heave motion at heading 70º, and Fig. 7 and Fig. 8 are PSD of surge and heave motion at heading 242º. In these figures, the dashed lines represent PSD from buoy data, and the solid lines are PSD of corresponding motion at center of gravity after filter method. Here, an offset vector of [0.5, 0, 1.9] was applied.
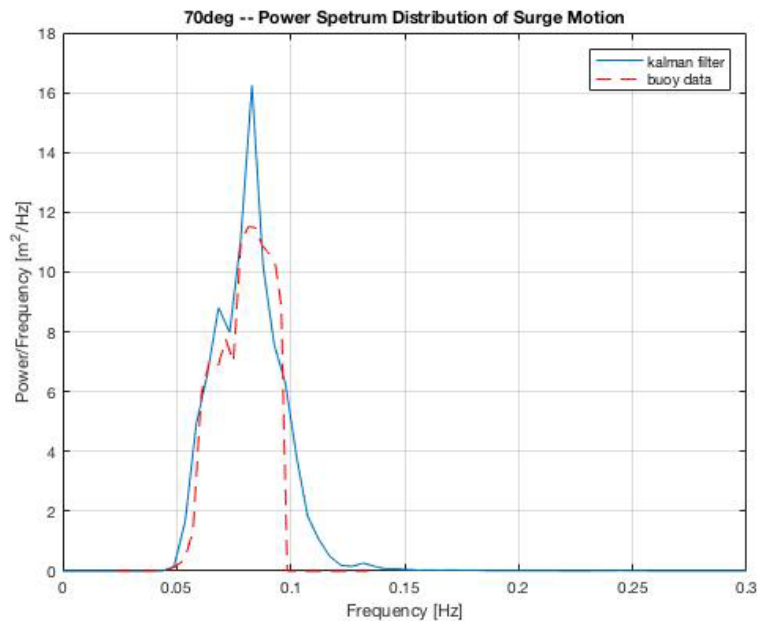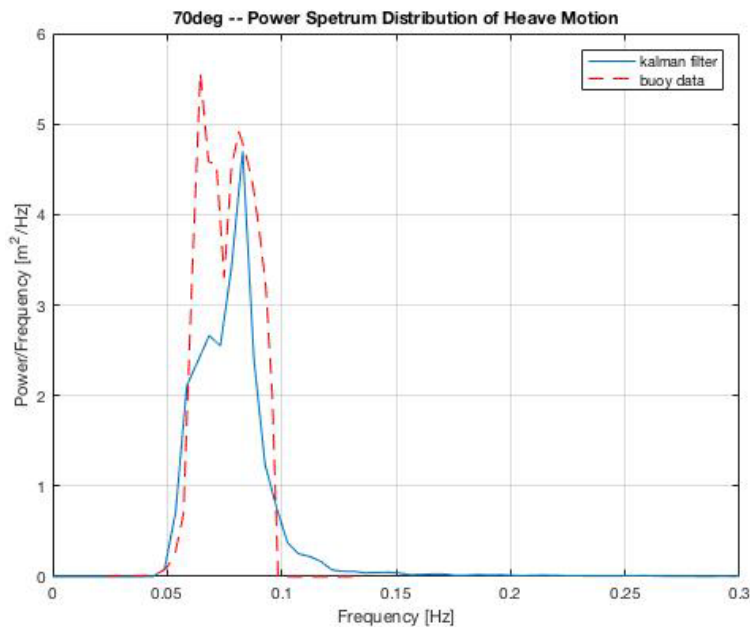

Fig. 5 Surge motion PSD at heading angle of 70º
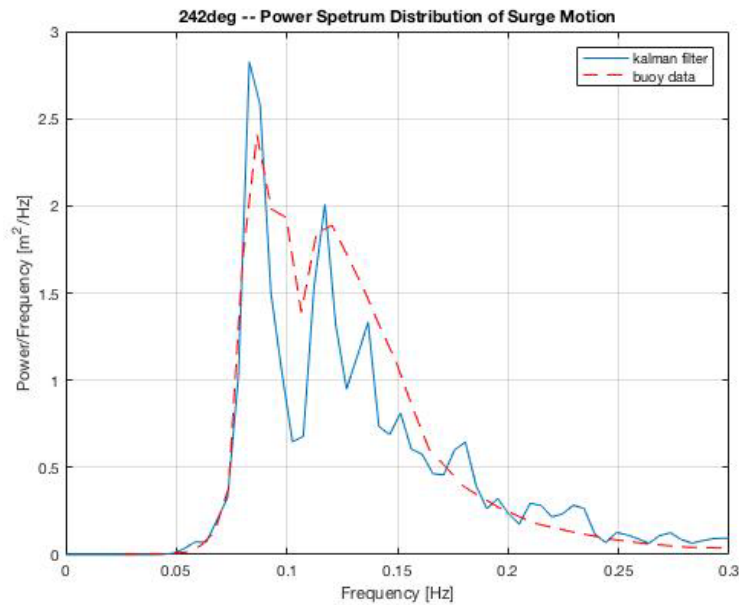

Fig. 6 Heave motion PSD at heading angle of 70º

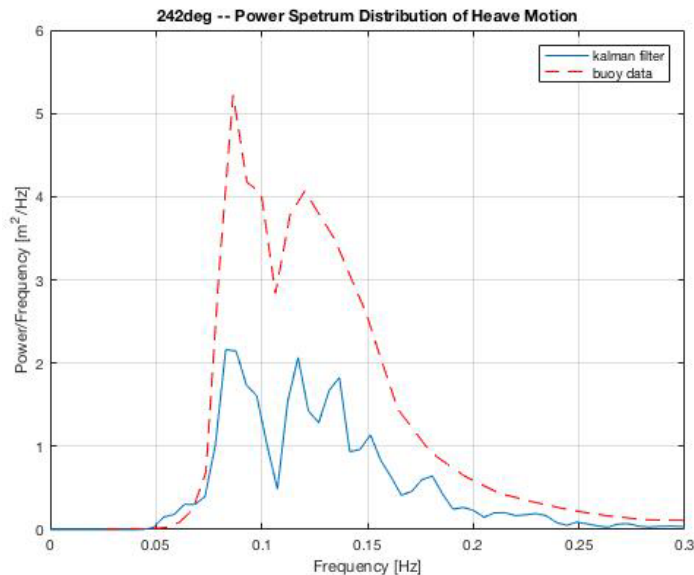Fig. 7 Surge motion PSD at heading angle of 242º

Fig. 8 Heave motion PSD at heading angle of 242º

B. Analysis and Discussion

Calculations were made for several different offset vectors and it turned out that heave is affected very little. This is probably due to a phase shift between heave and pitch tending to cancel the influence. For surge, a stronger effect is observed but, with the available data, the sensitivity is not enough to determine an offset vector uniquely. The offsets used in the figures correspond to the values estimated from the sensor position in the ship's plan.

As the waves' peak direction was 220° the ship is heading into the waves at 242˚, whereas at a heading of 70˚ the waves are following. In the latter case, we enter the region of ambiguous encounter frequencies explained in Fig. 2. Since

this ambiguity is difficult to resolve, the region had to be excluded from the RAOs and the expected spectra in Figs. 5 and 6 drop sharply above 0.1 Hz. Also, the wave buoy frequencies are shifted to lower encounter frequencies in Figs. 5 and 6, while in Figs. 7 and 8 they are pushed to higher encounter frequencies. In all cases, the observed frequencies match the expected ones closely.

Comparing the spectra in magnitude, a good fit can be observed for surge. Regarding heave, the spectra fit better at 70˚ than at 242˚, where the correspondence cannot be called satisfactory. The heave RAO seems beyond doubt, as it is close to unity up to about 0.2 Hz, and the offset vector has very little influence. So, the reason for the poor fit in Fig. 8 remains to be

investigated.

VII. Conclusion and Outlook

It is shown that measurements of the three accelerations and the three angular rates at one single point at an arbitrary position of the vessel are sufficient to calculate the CG motions. The spectra for heave and surge generally agree reasonably well with the predictions calculated from wave-buoy spectra, the exception for heave at head seas is discussed above. The reasons for the discrepancy are yet unclear. It is shown that a Kalman filter with a very simple system model is sufficient to calculate the CG motions. While a more sophisticated system model might lead to better noise reduction, the simple model is preferred because no previous knowledge of ship parameters for stability, damping or inertia are required for proper operation. The estimates of the sensor offset to the CG from measured data did not yield unique results in the current sea trials, mainly due to the rather small pseudo forces on the relatively small vessel. Data from trial runs on larger vessels will soon be available.

References

[1] Thor I. Fossen, Handbook of Marine Craft Hydrodynamics and Motion Control, 2011, ch.2.
[2] W. G. Price, R. E. D. Bishop, Probabilistic Theory of Ship Dynamics, 1974, ch.9.
[3] Gabriel A. Terejanu, Extended Kalman Filter Tutorial.
[4] L. M. Ehrman, A. D. Lanterman, "Extended Kalman Filter for Estimating Aircraft Orientation from Velocity Measurements", IET Radar Sonar Navigation, Vol.2, No.1, February 2008, pp.12–16.
[5] Dah-Jing Jwo, Sheng-Hung Wang, "Adaptive Fuzzy Strong Tracking Extended Kalman Filtering for GPS Navigation", IEEE Sensors Journal, Vol.7, No.5, May 2007, pp. 778-789.
[6] PDStrip, Program, 2006, https://sourceforge.net/projects/pdstrip.
[7] Volker Bertram, Alberto Alvarez, "Hydrodynamic Aspects of AUV Design", 5th International Conference on Computer Applications and Information Technology in the Maritime Industries, 8–10 May, 2006, pp. 45–53.
[8] Kai Graf, Marcus Pelz, Volker Bertram, H.Söding, "Added Resistance in Seaways and its Impact on Yacht Performance", 18th Chesapeake Sailing Yacht Symposium, March 2007.
[9] B. Schwarz-Röhr, B. NtambaNtamba, A. Härting, "Extending Sea State Measurements from Wave Buoys to Vessels Underway", Developing Sustainable Hydrography in Africa, Hydro Conference, November, 2015, pp. 11-20.